UNIVERSAL WISER
PUBLISHER

Article

Dynamic State Estimation of Synchronous Machines Using Iterated Square-Root Cubature Kalman Filter and Synchrophasor Measurements

Teena Johnson, Sofia Banu and Tukaram Moger

Department of Electrical & Electronics Engineering, National Institute of Technology Karnataka, Surathkal, Mangalore, 575025, India
E-mail: teenaj2007@gmail.com

Abstract: Power system dynamic state estimation is the first prerequisite for control and stability prediction under transient conditions. For a stable and reliable power system, it is crucial and helpful to have accurate, precise, and up-to-date information on the states of the synchronous machines- rotor angle and rotor speed deviation. This paper proposes an application of the Iterated Square-root Cubature Kalman filter (ISCKF) to estimate these main states of synchronous generators. The ISCKF method consists of two step modification - one is the square-root step modification of CKF and the next step is the addition of iterative approach to the square-root CKF method. To demonstrate the performance of the proposed approach during a three-phase short circuit fault, the simulation results, are compared with that of Extended Kalman Filter (EKF), Unscented Kalman Filter (UKF) and Cubature Kalman Filter (CKF). The test systems considered are a single machine infinite bus (SMIB) system, an IEEE 9-bus system and a 19-generator 42-bus test system. The estimation accuracy of the rotor angle using ISCKF method is increased by 6.8–36.54% when compared to that of the CKF method. Similarly, the improvement in accuracy is 4.4–28.57% for estimation of speed deviation.

Keywords: dynamic state estimation, synchronous machine, extended Kalman filter, unscented Kalman filter, cubature Kalman filter, iterated square-root cubature Kalman filter

1. Introduction

Electromechanical dynamic models are widely employed in power systems to examine transient and small-signal stability concerns. A dynamic model with appropriate known states may be used to anticipate and display system behaviour with accuracy, and boost power system stability. By utilising synchronised phasor measurement unit (PMU) readings, power system dynamic state estimation (PSDSE) calculates the states (such as rotor speeds and angles) of the system.

Researchers have explored several estimation techniques to investigate PSDSE. Extended Kalman Filter (EKF) was applied to PSDSE using second order model of the synchronous generator [1]. Evaluation of an EKF based estimator for power system considering lack of field voltage has been explored [2]. Dynamic state estimation (DSE) of synchronous machines in power system was carried out with the help of EKF [3]. The generator swings were observed for the three-phase fault case and load variation. This had further scope for identification of coherent group of generators in the system with the PMU measurements and help in adaptive protection of the system. Although EKF is a recursive update variant of Kalman filter that is computationally effective, it works best only in a mild non-linear conditions, as it is order-I Taylor series approximation of non-linear formulation [4]. It is seen to be inadequate and is prone to divergence. The linearization is only feasible if the Jacobian matrix exists. Nonetheless, determining Jacobian matrix might be difficult and error-prone. When

the system is highly non-linear, EKF tends to have very poor performance in precise estimation as it is based on first order Taylor approximation. While Unscented Kalman Filter (UKF) may attain upto order-III Taylor approximation for a non-linear system. The unscented transformation was designed to overcome EKF's linearization difficulty, by offering a more straight-forward and explicit approach for altering mean and covariance data. UKF was designed for PSDSE with PMU installed on generator bus [5]. A two-axis order-IV state space model of the synchronous generator is employed in this study. UKF was applied to various power system cases using order-II synchronous generator model while utilising the machine's speed and electric power generated as input measurements [6,7]. However, since UKF is dependent on the sigma-point set, the mean is highly influential as it given high weightage which proves to be unfavourable for high-dimensional systems. Therefore, UKF may encounter numerical instability troubles when used in high-dimensional problems.

For the purpose of PSDSE of the generator rotor angle in a large power system, a divide-by-difference-filter based method was presented [8]. When considering non-Gaussian noise, the extended particle filter's results for PSDSE in a single machine infinite bus (SMIB) system were compared to those of particle filters, EKF and UKF [9]. Data-driven DSE using artificial neural networks [10] and operator theory [11] have been explored in literature. A hybrid-learning dynamic state estimator was used for estimating the electromechanical states of power system [12]. Three-phase line trip faults were considered during the study. The hybrid-learning DSE is a data-driven approach using a power system model and by training neuroestimators with real time data. Pros and cons of this approach when compared to EKF and square-root UKF were presented. The applications and implementation of DSE with respect to modelling, monitoring and operation of power system were highlighted in [13]. The DSE for synchronous machines and converter-based resources have been explored [14]. Further, comparison studies were carried out for Kalman filter based approaches and observers for DSE based control and protection.

Cubature Kalman Filter (CKF) [15] employs a more precise cubature process to calculate Gaussian-weighted integrals, which is employed for PSDSE [16]. CKF requires error covariance matrix to be positive definite in every update, otherwise it can prevent the CKF from running continuously. A robust CKF was proposed for handling unknown noise characteristics in the measurement data [17]. In this work, Huber's M-estimation theory was incorporated into the original CKF approach. Comparison studies were carried for different types of noises. The estimated plots of rotor angle and speeds using robust CKF was found to be closer and overlapping with the actual/true plots when compared to CKF. In a recent paper [18], square-root cubature Kalman filter has been proposed for dynamic SE problem by integrating the Brown's double exponential smoothing technique at the prediction step. This method is compared to conventional EKF and CKF methods under normal and anomaly operating conditions. It was found to be a versatile method in scenarios of normal operating condition, in presence of bad data and load variations. The SCKF has been explored for estimation of dynamic time-varying coefficients related to rotating machines [19]. Nonetheless, there is application of square-root cubature Kalman filter (SCKF) performed for estimating state-of-charge in batteries [20].

The contributions of this paper can be summarized into the following points:

1. An alternative method devised in literature [21] for another estimation problem in space surveillance system used for space target tracking, which could be utilized for our application is identified. That is, a modified version of CKF called an Iterated Square-root Cubature Kalman filter (ISCKF) where it was demonstrated that ISCKF outperforms the conventional filters.

2. The ISCKF method consists of two step modification - one is the square-root step modification of CKF and the next step is the addition of iterative approach to the square-root CKF method.

   - Square-root CKF [15] approach that differs from CKF approach, as the square-root of error covariance matrix is determined by QR decomposition instead of Cholesky decomposition. Thereby, ISCKF eliminates the hazardous situation of the loss of positive definiteness of error covariance matrix in each update step, which could stop the UKF and CKF from running continuously.

   - Newton-Gauss iterative method was incorporated into the measurement update step of the square-root CKF for implementing the proposed ISCKF approach. Thus, improving the estimation accuracy.

3. In this paper, ISCKF is designed for its best use in PSDSE. The performance evaluation is carried out by implementing this proposed filter ISCKF to estimate the rotor speeds and angles of synchronous generators in SMIB, IEEE 9-Bus and 19-generator 42-bus test systems. The simulation results with respect to the accuracy in estimation (mean of absolute errors) of rotor speeds and angles are compared with those obtained using the existing DSE algorithms such as EKF, UKF and CKF.

The state estimation modelling using a classical generator model is described in Section 2. The ISCKF algorithm details are specified in Section 3. The Section 4 delves into how simulation results and observations were carried out for the study using the test systems. Section 5 presents conclusion based on the results obtained for the proposed estimator and the other dynamic state estimators considered.

2. Modeling and Problem Formulations

Rotor angle and rotor speed deviation are estimated using the classical model of synchronous generator.

$$\dot{\delta} = \omega_0 \Delta\omega$$
$$\Delta\dot{\omega} = \frac{1}{2H}(P_m - P_e - D\Delta\omega) \tag{1}$$

where δ - rotor angle in radian; $\Delta\omega$ - rotor speed deviation, P_m - mechanical power and P_e - electric air gap power. ω_0 - rated angular frequency; H - inertia constant; and D - damping coefficient. For generalization, (1) is transformed into a state space model as follows

$$\dot{x} = f_c(x, u) + \omega_c \tag{2}$$

$$y = h_c(x, u) + v_c \tag{3}$$

$$E\left[\omega_c \omega_c^T\right] = Q \tag{4}$$

$$E\left[v_c v_c^T\right] = R \tag{5}$$

$$x = \left[\delta, \Delta\omega\right]^T \tag{6}$$

$$u = \left[P_m\right]^T \tag{7}$$

$$y = \left[P_t\right]^T \tag{8}$$

In (2) and (3), x, u, y - state, input and output vectors respectively; $f_c(*)$ and $h_c(*)$ - state transformation and output functions respectively; subscript "c" stands for continuous time formulation; ω_c, v_c - process and output noise vectors respectively. ω_c and v_c represent Gaussian white noises with covariance matrices defined by (4) and (5) as Q and R. $E[*]$ - statistical expectation. The above expressions are converted to discrete form utilizing modified Euler's method [22] due to the inherent discrete nature of measurements [9].

All filtering algorithms use state estimation model, which is introduced in this section. We know that the simulation model may be different from the estimation model, simulation model is for mimicking system behaviours while an estimation model is for estimating states.

3. Iterated Square-Root Cubature Kalman Filter

The proposed ISCKF improves the accuracy and numerical stability of the square-root cubature Kalman filter [21] by including a Newton-Gauss iterative technique [23,24] into the measurement update step as elaborated in the algorithm description below.

3.1 Algorithm

The algorithm of the proposed ISCKF is described in the following steps.
Time Update:
1. Evaluate the cubature points ($i = 1, 2, ... m$)

$$X_{i,\,k-1|k-1} = S_{k-1|k-1}\xi_i + \hat{x}_{k-1|k-1} \tag{9}$$

where $m = 2n_x$ and n_x is the number of states. When $k = 1$

$$S_{0|0} = sqrt(P_0) \tag{10}$$

2. Evaluate propagated cubature points ($i = 1, 2, \ldots m$)

$$X_{i, k-1|k-1}^* = f\left(X_{i, k-1|k-1}\right) \tag{11}$$

where $f(X)$ is given in (2).

3. Estimate predicted state

$$\hat{x}_{k|k-1} = \frac{1}{m}\sum_{i=1}^{m} X_{i, k|k-1}^* \tag{12}$$

4. Estimate the square-root factor of the predicted error covariance

$$S_{k|k-1} = Tria\left(\left[X_{k|k-1}^*, S_{Q, k-1}\right]\right) \tag{13}$$

where $S_{Q, k-1}$ denotes a square-root factor of Q_{k-1}, such that $Q = S_{Q, k-1}S_{Q, k-1}^T$, and $X_{k|k-1}^*$ defined as

$$x_{k|k-1}^* = \frac{1}{\sqrt{m}}\left[X_{1, k|k-1}^* - \hat{x}_{k|k-1}, X_{2, k|k-1}^* - \hat{x}_{k|k-1} \cdots X_{m, k|k-1}^* - \hat{x}_{k|k-1}\right] \tag{14}$$

Measurement Update:

1. Evaluate cubature points ($i = 1, 2, \ldots m$)

$$X_{i, k-1|k-1}^{(j)} = \hat{S}_{k-1|k-1}(j)\xi_i + \hat{x}_{k|k-1}^{(j)} \tag{15}$$

where $= 0, 1, \ldots$ (internal iteration count) for ISCKF and when $= 0$, $\hat{S}_{k|k-1}^{(0)} = S_{k|k-1}$ and $\hat{x}_{k|k-1}^{(0)} = \hat{x}_{k|k-1}$

2. Evaluate propagate cubature points ($i = 1, 2, \ldots m$)

$$Z_{i, k|k-1}^{(j)} = h\left(X_{i, k|k-1}^{(j)}\right) \tag{16}$$

3. Estimate the predicted measurement

$$\hat{z}_{k|k-1}^{(j)} = \frac{1}{m}\sum_{i=1}^{m} Z_{i, k|k-1}^{(j)} \tag{17}$$

4. Estimate the square-root of the innovation covariance matrix

$$S_{zz, k|k-1}^{(j)} = Tria\left[Z_{k|k-1}^{(j)}, S_{R, k}^{(j)}\right] \tag{18}$$

where $S_{R, k}^{(j)}$ denotes a square-root factor of $R_k^{(j)}$ such that $R_k^{(j)} = S_{R, k}^{(j)}\left(S_{R, k}^{(j)}\right)^T$ and $Z_{k|k-1}^{(j)}$ is defined as

$$Z_{k|k-1}^{(j)} = \frac{1}{\sqrt{m}}\left[Z_{1, k|k-1}^{(j)} - \hat{z}_{k|k-1}^{(j)}, Z_{2, k|k-1}^{(j)} - \hat{z}_{k|k-1}^{(j)} \cdots Z_{m, k|k-1}^{(j)} - \hat{z}_{k|k-1}^{(j)}\right] \tag{19}$$

5. Estimate the cross-covariance matrix

$$P_{xz, k|k-1}^{(j)} = X_{k|k-1}\left(Z_{k|k-1}^{(j)}\right)^T \tag{20}$$

where $X_{k|k-1}$ is defined as

$$x_{k|k-1}^{(j)} = \frac{1}{\sqrt{m}}\left[X_{1, k|k-1}^{(j)} - \hat{x}_{k|k-1}^{(j)}, X_{2, k|k-1}^{(j)} - \hat{x}_{k|k-1}^{(j)} \cdots X_{m, k|k-1}^{(j)} - \hat{x}_{k|k-1}^{(j)}\right] \tag{21}$$

6. Estimate the Kalman gain

$$P_{zz, k|k-1}^{(j)} = S_{zz, k|k-1}^{(j)}\left(S_{zz, k|k-1}^{(j)}\right)^T \tag{22}$$

$$W_k^{(j)} = \frac{P_{xz,\,k|k-1}^{(j)}}{\left(P_{zz,\,k|k-1}^{(j)} + R_k^{(j)}\right)} \tag{23}$$

7. Estimate the updated state

$$\hat{x}_{k|k}^{(j)} = \hat{x}_{k-1|k}^{(j)} + W_k^{(j)}\left(z_k^{(j)} - \hat{z}_{k|k-1}^{(j)}\right) \tag{24}$$

8. Estimate the square-root factor of the corresponding error covariance

$$S_{k|k}^{(j)} = Tria\left[\chi_{k|k-1}^{(j)} - W_k^{(j)}Z_{k|k-1}^{(j)}, W_k^{(j)}S_{R,k}^{(j)}\right] \tag{25}$$

9. Make $\hat{x}_{k|k-1}^{(j+1)} = \hat{x}_{k|k}^{(j)}$, $S_{k|k-1}^{(j+1)} = S_{k|k}^{(j)}$ and $j = j+1$.

Return to Measurement Update Step 1 and end for $j = N$.

The flowchart of the algorithm to show how the estimation and filtering process takes place using the actual data and ISCKF algorithm is illustrated in Figure 1.
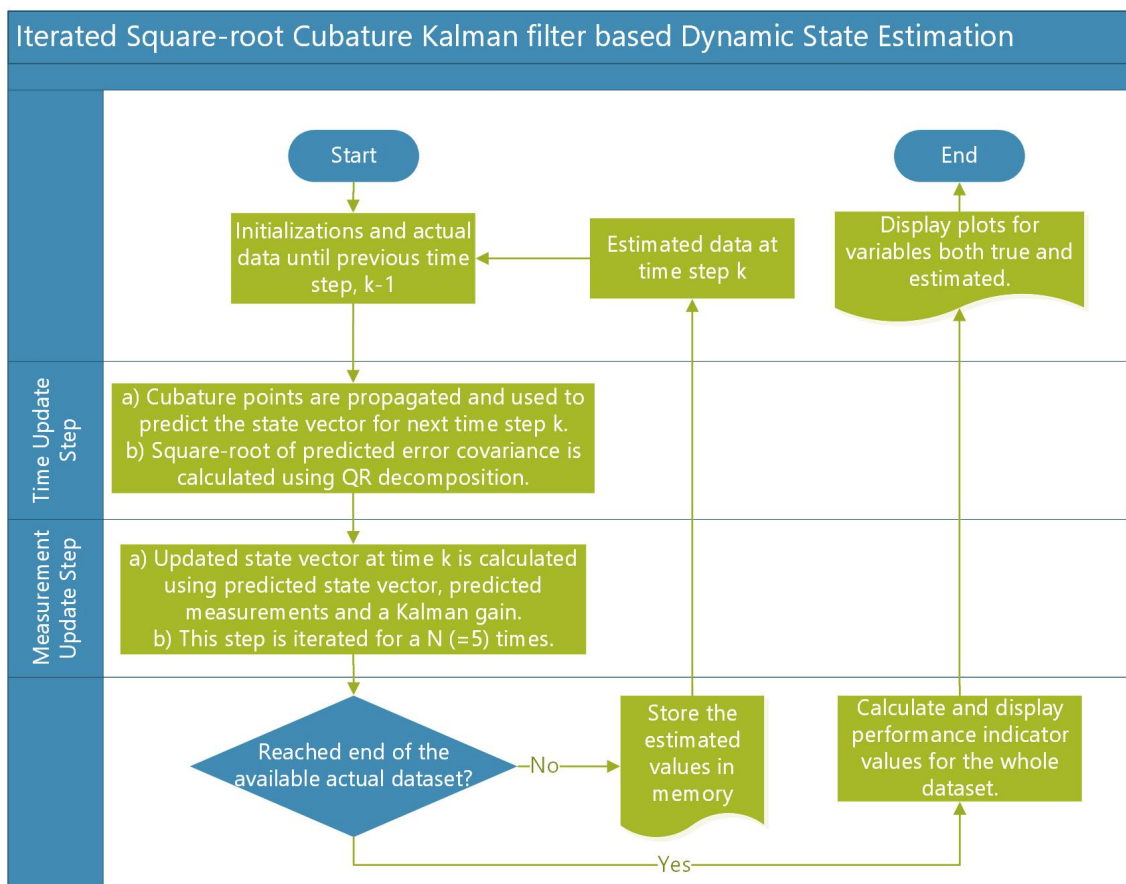

Figure 1. The flowchart for the general flow of logic in dynamic state estimation using Iterated square-root Kalman filter.

4. Simulations

To demonstrate the validity and reliability of the proposed algorithm, in this section ISCKF is implemented for DSE for the test systems considered in the subsequent subsections. The estimator algorithms ISCKF, CKF, UKF and EKF are coded in MATLAB© 2015a platform and run on Windows 10 with Intel core i5 with 8GB RAM.

Some initial parameters are defined as follows: the covariance of state process noise Q is a diagonal matrix $[10^{-6}, 10^{-2}]$, the covariance of the measurement noise $R = 0.001$, the initial states $\dot{x} = 0$, initial covariance $_0 = 10^{-3} \times I$. Here I is the identity matrix of size $n_x \times n_x$. of the internal iteration number N for ISCKF is set as 5. All the simulation data for state estimation is generated at 25 samples/s to mimic the PMU sampling rate. Adding

more measurements increases the efficient sampling rate, consequently minimising linearisation errors [25]. The sampling rate is enhanced from 25 to 1000 samples per second by utilising linear interpolation to insert extra pseudo measurements for every two measurement instants. As a consequence of the interpolation, the sampling time interval Δt is reduced from 40ms to 1ms. For simulating the practical PMU measurements, 5% of measurement noise added to the voltage and current phasors. The measurement noise includes the noises introduced by PMU device, current transformers and potential transformers.

4.1 *SMIB*

A compact equivalent model of a generic power system that consists of a single generator coupled to an infinite bus via parallel transmission lines and a transformer is simulated in PowerWorld Simulator [26]. The PowerWorld schematic of SMIB is given in Figure 2. The specified values used for the generator parameters are provided in Appendix: Table 5 with P_{base} = 100 MVA.
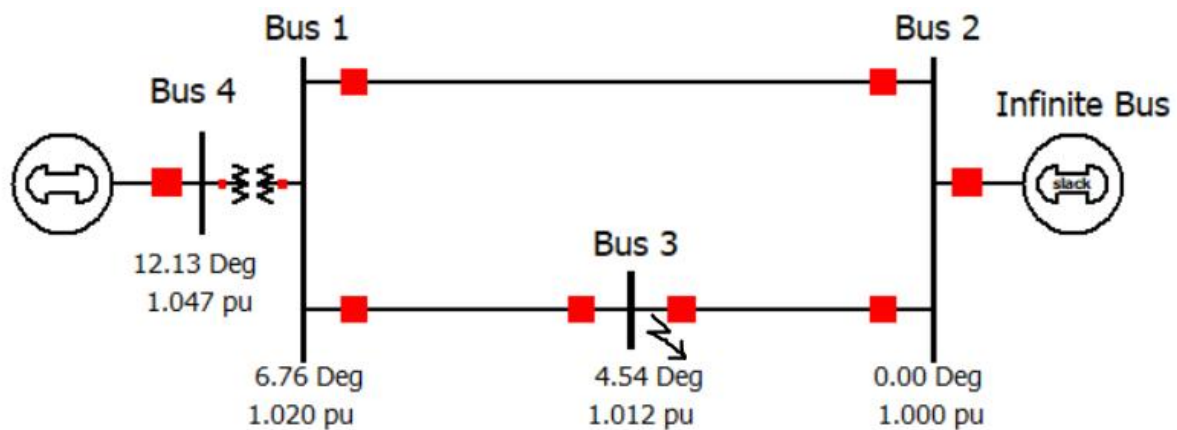

Figure 2. SMIB system.

The simulation scenario is a symmetrical permanent three-phase-to-ground bolted short circuit fault added to bus-3 at 1s and cleared by removing the line 1-3 and line 2-3 at 1.3s. Assuming the PMU is placed at the main generator. The simulation data of the main generator and bus is taken from the PowerWorld Simulator [26]. The simulation results for the main states, rotor angle and rotor speed deviation of the main generator estimated using ISCKF are compared with EKF, UKF and CKF are presented in Figure 3 and Figure 4 respectively.

From the Figures 3b and 4b, ISCKF is giving least error. The mean of absolute errors in the states and the estimation time per iteration are listed in the Table 1. From these results, it is observed that by using ISCKF, the accuracy in rotor angle estimation has increased by 6.82% and in speed deviation the estimation accuracy has increased by 4.44% that of CKF. The percentage increase in accuracy is calculated as follows:

$$\left| \frac{\text{MAE}_{ISCKF} - \text{MAE}_{CKF}}{\text{MAE}_{CKF}} \right| \times 100 \qquad (26)$$

Here, MAE (mean of absolute errors) is either with respect to rotor angle or rotor speed deviation of all the generators. And the estimation time per iteration is within the time next set of measurements arrive, that is 1ms for all the 4 types of estimators.

Table 1. Mean of Absolute Errors (MAE) in the Estimated States using SMIB test system.
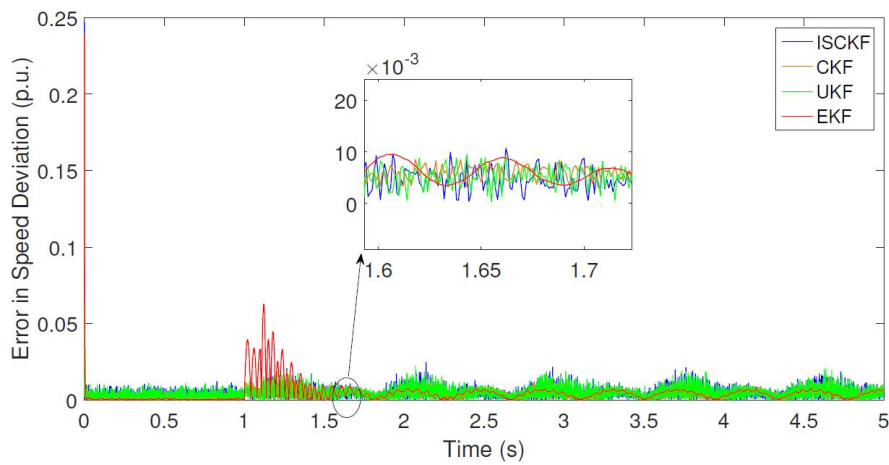
	MAE in Rotor Angle (rad.)	MAE in Speed Deviation (p.u.)	Estimation time per iteration (ms)
ISCKF	0.0041	0.0043	0.30
CKF	0.0044	0.0045	0.08
UKF	0.0060	0.0046	0.09
EKF	0.0801	0.0048	0.03

(a) Rotor angle plots

(b) Error in rotor angle
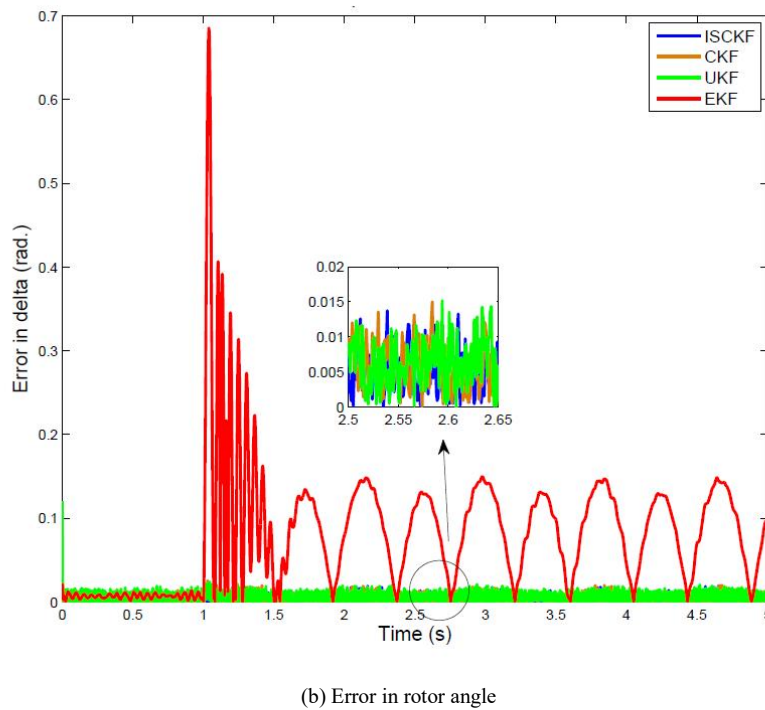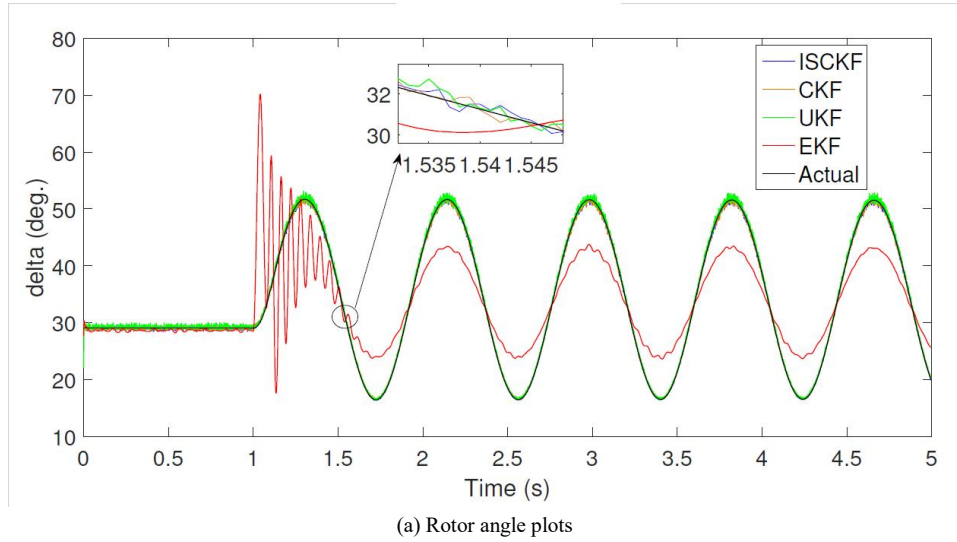
Figure 3. The estimated rotor angle and error plots at main generator bus for SMIB.
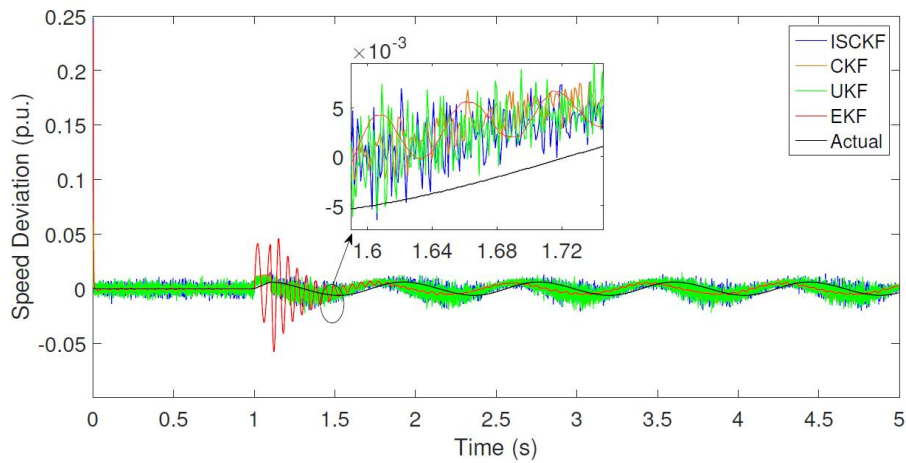
(a) Speed deviation plots

(b) Error in speed deviation

Figure 4. The estimated speed deviation and error plots for SMIB.

4.2 *IEEE 9-Bus System*

The case study is carried out on IEEE 9-bus system shown in Figure 5. The classical model as described in Section 2, is used to represent all generators in this system. To analyse the transient stability of a system with many machines, the initial conditions of the generators and buses must be determined. The power flow solution helps to determine the steady state voltages and angles of the buses. Together with the given values used for the generator parameters (Refer Appendix: Table 6), these steady state values are utilised as initial conditions for the simulation in Power World simulator.
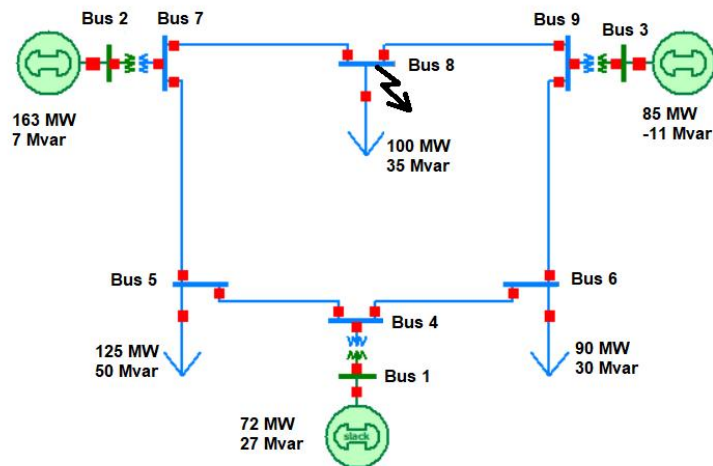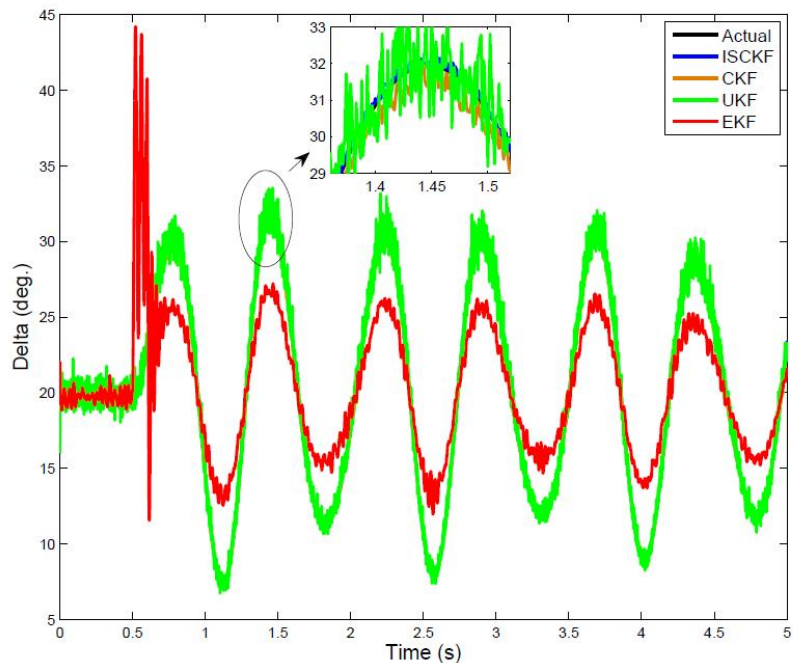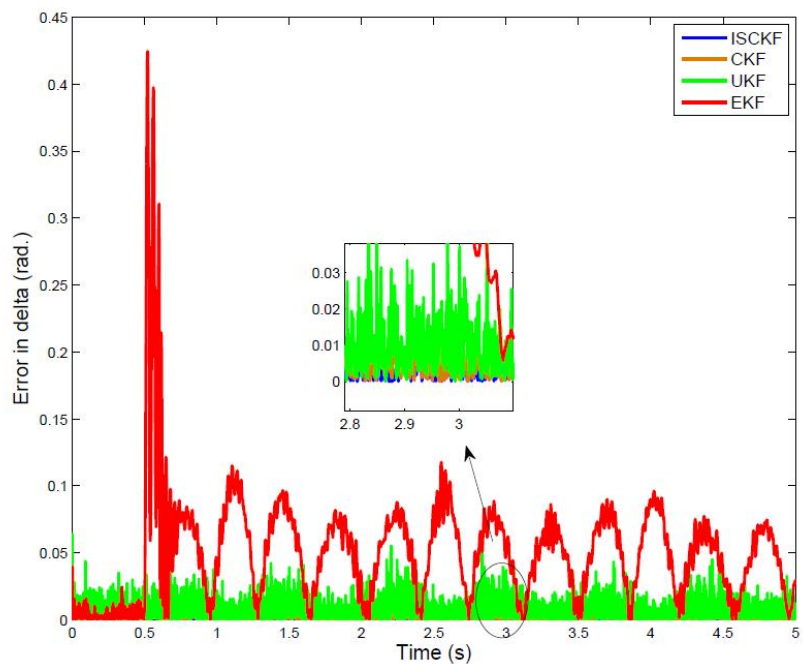

Figure 5. IEEE 9-Bus System.

The fault scenario considered for this case is a balanced three-phase to ground fault on Bus-8 at $t = 1s$ which is cleared at $t = 1.1s$ by removing the lines 7-8 and line 9-8. The PMU sampling rate of 25 samples per second is used in simulation data and linear interpolation is used to increase the effective sampling rate to 1000 samples per second.

For comparison of the ISCKF with EKF, UKF and CKF the estimation results of rotor angle, speed deviation and the corresponding error plots at generator bus-2 are given in Figure 6 and Figure 7. The mean of absolute errors in the estimated states and the estimation time per iteration and the estimation time per iteration are listed in Table 2.
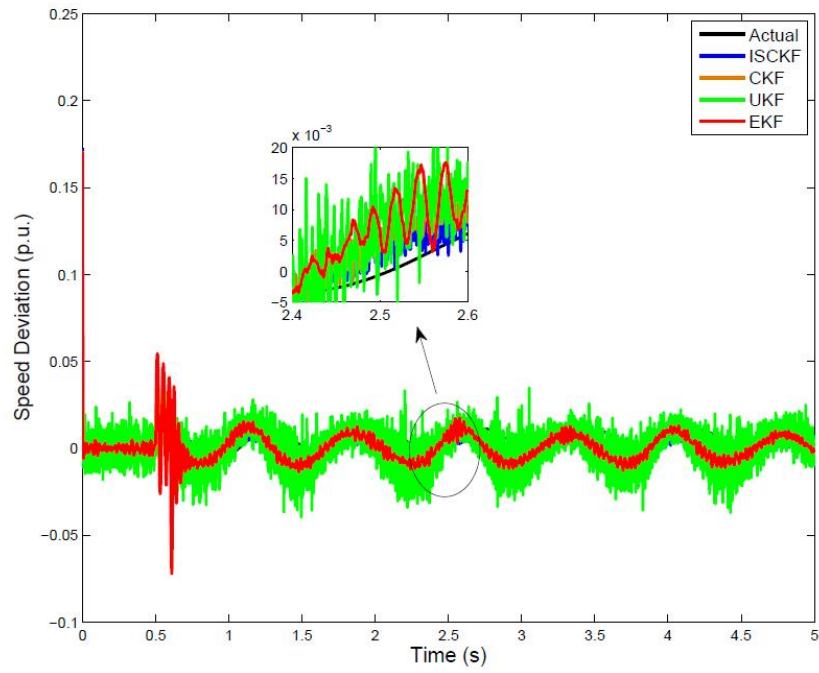

(a) Rotor angle plots

(b) Error in rotor angle

Figure 6. The estimated rotor angle and absolute error plots at generator bus-2 for IEEE 9-bus system.

(a) Speed deviation plots
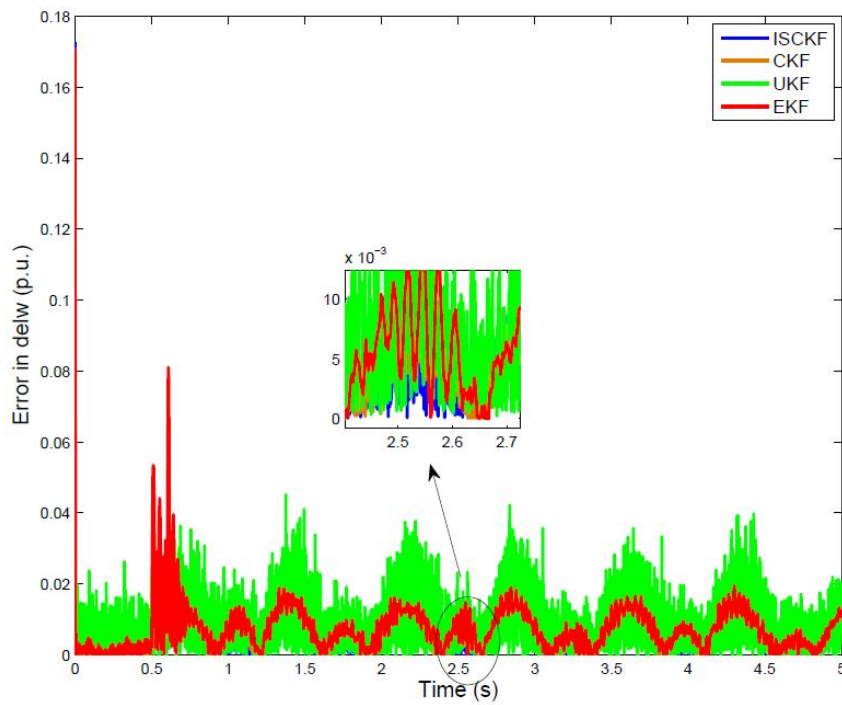
(b) Error in speed deviation

Figure 7. The estimated speed deviation and absolute error plots at generator bus-2 for IEEE 9-bus system.

Table 2. Mean of Absolute Errors (MAE) in the Estimated States at all generator buses in IEEE 9-bus system.

	MAE in Rotor Angle (rad.)	MAE in Speed Deviation (p.u.)	Estimation time per iteration (ms)
ISCKF	0.0019	0.0088	0.80
CKF	0.0022	0.0097	0.30
UKF	0.0026	0.0098	0.20
EKF	0.0025	0.0102	0.06

From the results and the mean of absolute errors, it can be observed that the MAE in rotor angle estimation using ISCKF is 0.0019 rad. Therefore, there is an increased accuracy of 13.64% in rotor angle estimation with respect to that obtained using CKF. Similarly, the MAE in speed deviation using ISCKF is 0.0088 p.u., implies increased accuracy of 9.28% in speed deviation estimation when compared to that obtained using CKF. ISCKF is proved to be more accurate for the state estimation in the multi-machine system as well. And the estimation time per iteration is within the time next set of measurements arrive, that is 1ms for all the 4 types of estimators.

4.3 19-Generator 42-bus Test System

The 19-generator 42-bus test system data is generated using the existing script files "*case19l*" and "*s_simu*" in *psdat* and *pstv2* folders of Power System toolbox version 2 [27]. MATLAB© R2015a platform is used to run and generate the data for state estimation. The system details utilized from "*case19l*" script file are provided in Appendix: Table 7. The simulation scenario is a three-phase fault applies at bus-30 at 1.0s and is cleared by removing the line at 1.1s. For simulation, the sampling time is taken as typical PMU reporting rate 25 samples per second linearly interpolated to 1000 samples per second as considered in previous system simulations. As a consequence of the interpolation, the sampling time interval Δt for the input and measurement data is reduced from 40ms to 1ms. From the tabulated errors in the Table 3, it is observed that by using ISCKF, the accuracy in the rotor angle estimations is increased by 29.41%and the accuracy in the speed deviation estimation has increased by 22.95% than that obtained by CKF. But it has been observed that the estimation time per iteration is exceeding 1ms for ISCKF, CKF and UKF estimators (See Table 3). That is, the estimation is not being performed before the arrival of next set of measurements. For this larger system, as the estimation process involves large number of variables, a trade-off has to be made between the samples per second of measurement data and the number of variables in the estimation process. The only part which can be modified is samples per second of measurement data, by using down-sampling technique. Hence, 250 samples per second is chosen, to make the estimation process feasible within the arrival time of next set of measurement, by interpolating 25 samples per second to 250 samples per second. Also, the number of internal iterations count N of ISCKF has been reduced to 3 instead of 5 (which has been used in smaller systems discussed in previous sub-sections). Now, the results after these changes are noted in Table 4 showing that the estimation time per iteration is within 4ms for all types of estimators. Thus, can be implemented for real-time online DSE. Further if the measurement data are considered at the rate 250 samples per second (See Table 4), the accuracy of state estimations by ISCKF is the best among all. The accuracy in the rotor angle estimations by ISCKF is increased by 36.54% than that of CKF. While the accuracy in the speed deviation estimation by ISCKF has increased by 28.57% than that of CKF. The estimation results obtained at generator bus-6 with 250 samples per second input and measurement data is shown in Figure 8 and Figure 9. The mean of the absolute errors in estimation of states at all the generator buses using different filters is tabulated in the Table 4.

Table 3. Mean of Absolute Error (MAE) in the Estimated States of all generator buses of 42-bus test system (Measurement data: 1000 samples/s).

	MAE in Rotor Angle (rad.)	MAE in Speed Deviation (p.u.)	Estimation time per iteration (ms)
ISCKF	0.0036	0.0047	3.1
CKF	0.0051	0.0061	1.8
UKF	0.0050	0.0070	1.8
EKF	0.1845	0.0052	0.5

Table 4. Mean of Absolute Error (MAE) in the Estimated States of all generator buses of 42-bus test system (Measurement data: 250 samples/s).

|	MAE in Rotor Angle (rad.)	MAE in Speed Deviation (p.u.)	Estimation time per iteration (ms)
ISCKF	0.0033	0.0045	3.7
CKF	0.0052	0.0063	1.6
UKF	0.0051	0.0070	1.7
EKF	0.1525	0.0108	0.5

When the results of Tables 1, 2 and 3 are compared, it can be observed that with increase in number of generator buses from 1 to 19 in the system, though the computational time increases almost linearly, the MAE is almost the same and hence estimation accuracy is consistently good.

Since the proposed method has repetitive iterations within the state update step, the computational time is higher than the other methods as observed in Tables 1, 2 and 3. But the accuracy is improved significantly and hence is advantageous. The increase in estimation time for the first two test system SMIB system and IEEE 9-bus system is well within the arrival time of next set of data and hence does not adversely affect the estimator performance.

(a) Rotor angle plots

(b) Error in rotor angle
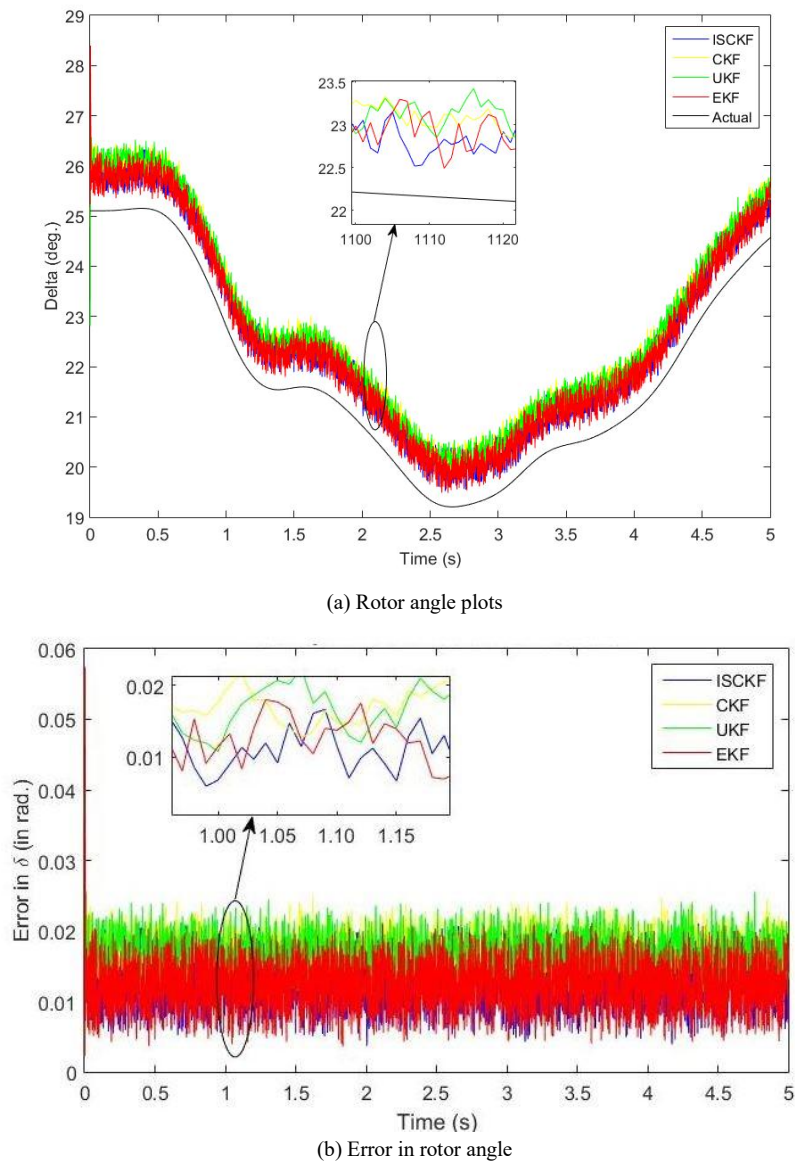
Figure 8. The rotor angle and error plots at generator bus-6 in 19-gen 42-bus test system.
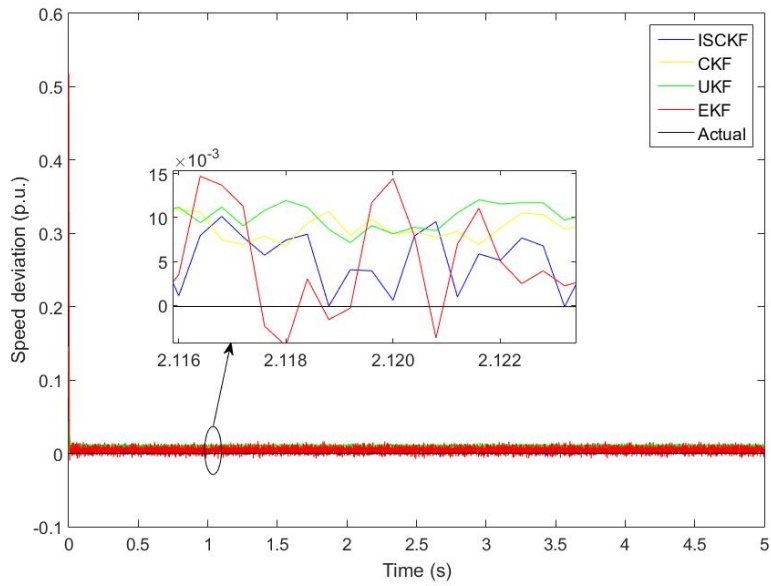
(a) Speed deviation plots
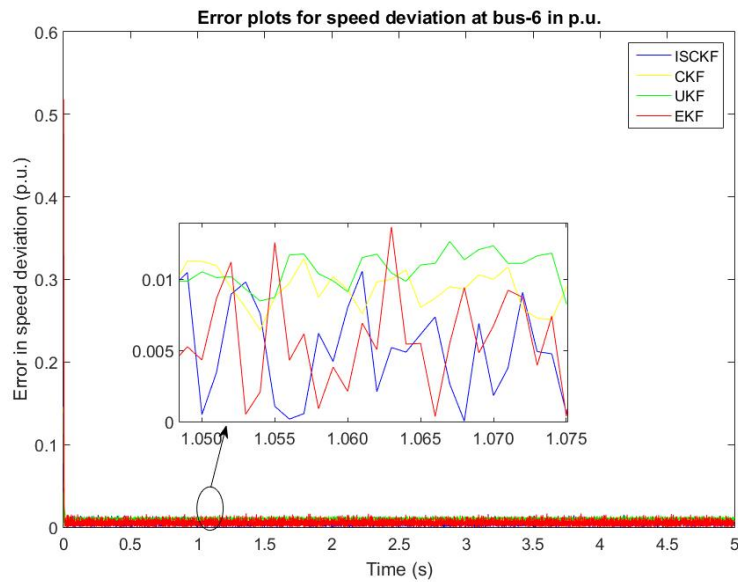
(b) Error in speed deviation

Figure 9. The estimated speed deviation and error plots at generator bus-6 in 19-gen 42-bus test system.

5. Conclusions

For best possible monitoring and control of complex systems such as our electric power grids, dynamic system modelling and state estimation are required. In addition to noise rejection, an estimator employs a system's state space model to offer information on the system's states, which are sometimes immeasurable. In this study, the mathematical state space modelling is utilized for dynamic state estimation using non-linear Kalman Filters. Preliminary studies are carried out for speed estimation process of an induction motor using the existing Extended, Unscented and Cubature Kalman filter versions. The simulation results of this section show the capability of the proposed approaches to estimate the speed optimally even with the added noisy measurements. Further, classical model of the synchronous generator is used to model single machine infinite bus system and then large multi-machine power systems (such as IEEE 9-bus and 19-generator 42-bus test systems). Iterated square-root cubature Kalman filter (ISCKF) based state observer design is proposed for the dynamic state estimation of rotor angle and speed of synchronous machines in power systems. Theoretically, ISCKF approach eliminates the hazardous situation of the loss of positive definiteness of error covariance

matrix in each update step which can stop the UKF and CKF from running continuously. Through the simulation studies carried out during a three-phase short circuit fault, the performance comparison of ISCKF is carried out with the existing methods such as EKF, UKF and CKF. It is clearly evident that the accuracy of state estimations is improved greatly when compared to that of EKF, UKF and CKF. At the measurement data rate of 250 samples per second, the estimation time per iteration is within the time 4ms, i.e., before the next set of measurements arrives. Therefore, it can be implemented for online dynamic state estimation for synchronous machines in a power system. For smaller systems such as SMIB and IEEE 9-bus systems, higher sampling rate of 1000 samples per second for measurement data, further improves the accuracy of estimation.

Conflict of Interest

There is no conflict of interest for this study.

References

[1] Huang, Z.; Schneider, K.; Nieplocha, J. Feasibility studies of applying kalman filter techniques to power system dynamic state estimation. In Proceedings of 2007 International Power Engineering Conference (IPEC 2007), Singapore, 3–6 December 2007. pp. 376–382.

[2] Ghahremani, E.; Kamwa, I. Dynamic State Estimation in Power System by Applying the Extended Kalman Filter with Unknown Inputs to Phasor Measurements. *IEEE Trans. Power Syst.* **2011**, *26*, 2556–2566, https://doi.org/10.1109/tpwrs.2011.2145396.

[3] Pan, P.; Sharma, M.K.; Ghose, T.; Mohanta, D. Synchrophasor based concurrent swing and state estimation of synchronous generator. In Proceedings of 2018 Technologies for Smart-City Energy Security and Power (ICSESP), Bhubaneswar, India, 28–30 March 2018, https://doi.org/10.1109/icsesp.2018.8376701.

[4] Zhou, N.; Meng, D.; Huang, Z.; Welch, G. Dynamic State Estimation of a Synchronous Machine Using PMU Data: A Comparative Study. *IEEE Trans. Smart Grid* **2014**, *6*, 450–460, https://doi.org/10.1109/tsg.2014.2345698.

[5] Ghahremani, E.; Kamwa, I. Online State Estimation of a Synchronous Generator Using Unscented Kalman Filter from Phasor Measurements Units. *IEEE Trans. Energy Convers.* **2011**, *26*, 1099–1108, https://doi.org/10.1109/tec.2011.2168225.

[6] Wang, S.; Gao, W.; Meliopoulos, A.P.S. An Alternative Method for Power System Dynamic State Estimation Based on Unscented Transform. *IEEE Trans. Power Syst.* **2011**, *27*, 942–950, https://doi.org/10.1109/tpwrs.2011.2175255.

[7] Gao, W.; Wang, S. On-line dynamic state estimation of power systems. In Proceedings of North American Power Symposium 2010, Arlington, TX, USA, 26–28 September 2010, https://doi.org/10.1109/naps.2010.5619951.

[8] Tripathy, P.; Srivastava, S.C.; Singh, S.N. A Divide-by-Difference-Filter Based Algorithm for Estimation of Generator Rotor Angle Utilizing Synchrophasor Measurements. *IEEE Trans. Instrum. Meas.* **2009**, *59*, 1562–1570, https://doi.org/10.1109/tim.2009.2026617.

[9] Zhou, N.; Meng, D.; Lu, S. Estimation of the Dynamic States of Synchronous Machines Using an Extended Particle Filter. *IEEE Trans. Power Syst.* **2013**, *28*, 4152–4161, https://doi.org/10.1109/tpwrs.2013.2262236.

[10] Del Angel, A.; Geurts, P.; Ernst, D.; Glavic, M.; Wehenkel, L. Estimation of rotor angles of synchronous machines using artificial neural networks and local PMU-based quantities. *Neurocomputing* **2007**, *70*, 2668–2678, https://doi.org/10.1016/j.neucom.2006.12.017.

[11] Netto, M.; Mili, L. A Robust Data-Driven Koopman Kalman Filter for Power Systems Dynamic State Estimation. *IEEE Trans. Power Syst.* **2018**, *33*, 7228–7237, https://doi.org/10.1109/tpwrs.2018.2846744.

[12] Tian, G.; Zhou, Q.; Birari, R.; Qi, J.; Qu, Z. A Hybrid-Learning Algorithm for Online Dynamic State Estimation in Multimachine Power Systems. *IEEE Trans. Neural Networks Learn. Syst.* **2020**, *31*, 5497–5508, https://doi.org/10.1109/tnnls.2020.2968486.

[13] Zhao, J.; Netto, M.; Huang, Z.; Yu, S.S.; Gomez-Exposito, A.; Wang, S.; Kamwa, I.; Akhlaghi, S.; Mili, L.; Terzija, V.; et al. Roles of Dynamic State Estimation in Power System Modeling, Monitoring and Operation. *IEEE Trans. Power Syst.* **2020**, *36*, 2462–2472, https://doi.org/10.1109/tpwrs.2020.3028047.

[14] Liu, Y.; Singh, A.K.; Zhao, J.; Meliopoulos, A.P.S.; Pal, B.; Ariff, M.A.B.M.; Van Cutsem, T.; Glavic, M.; Huang, Z.; Kamwa, I.; et al. Dynamic state estimation for power system control and protection. *IEEE Trans. Power Syst.* **2021**, *36*, 5909–5921, https://doi.org/10.1109/tpwrs.2021.3079395.

[15] Arasaratnam, I; Haykin, S. Cubature kalman filters. *IEEE Trans. Automat. Control* **2009**, *54*, 1254–1269, https://doi.org/10.1109/TAC.2009.2019800

[16] Sharma, A.; Srivastava, S.C.; Chakrabarti, S. A Cubature Kalman Filter Based Power System Dynamic State Estimator. *IEEE Trans. Instrum. Meas.* **2017**, *66*, 2036–2045, https://doi.org/10.1109/tim.2017.2677698.

[17] Li, Y.; Li, J.; Qi, J.; Chen, L. Robust Cubature Kalman Filter for Dynamic State Estimation of Synchronous Machines Under Unknown Measurement Noise Statistics. *IEEE Access* **2019**, *7*, 29139–29148, https://doi.org/10.1109/access.2019.2900228.

[18] Basetti, V.; Chandel, A.K.; Shiva, C.K. Square-root cubature Kalman filter based power system dynamic state estimation. *Sustain. Energy, Grids Networks* **2022**, *31*, https://doi.org/10.1016/j.segan.2022.100712.

[19] Kang, Y.; Qiu, Z.; Fan, Q.; Zhang, H.; Shi, Z.; Gu, F. Tacholess estimation of time-varying dynamic coefficients of journal bearing based on the square-root cubature Kalman filter. *Measurement* **2022**, *203*, https://doi.org/10.1016/j.measurement.2022.111956.

[20] Chen, L.; Yu, W.; Cheng, G.; Wang, J. State-of-charge estimation of lithium-ion batteries based on fractional-order modeling and adaptive square-root cubature Kalman filter. *Energy* **2023**, *271*, https://doi.org/10.1016/j.energy.2023.127007.

[21] Wang, C.; Wu, P.; Deng, Y. Modified iterated square-root cubature kalman filter for non-cooperative space target tracking. *Int. J. Eng. Appl. Sci.* **2015**, *2*, 257789.

[22] Schinkel, M.; Heemels, W.; Juloski, A. State estimation for systems with varying sampling rate. In Proceedings of 42nd IEEE International Conference on Decision and Control (IEEE Cat. No.03CH37475), Maui, HI, USA, 9–12 December 2003, https://doi.org/10.1109/cdc.2003.1272593.

[23] Yang, Z.; Zhong, D.; Guo, F.; Zhou, Y. Gauss-newton iteration based algorithm for passive location by a single observer. *Syst. Eng. Electron.* **2007**, *29*, 2006–2009.

[24] Johnston, L.; Krishnamurthy, V. Derivation of a sawtooth iterated extended Kalman smoother via the AECM algorithm. *IEEE Trans. Signal Process.* **2001**, *49*, 1899–1909, https://doi.org/10.1109/78.942619.

[25] Akhlaghi, S.; Zhou, N.; Huang, Z. A Multi-Step Adaptive Interpolation Approach to Mitigating the Impact of Nonlinearity on Dynamic State Estimation. *IEEE Trans. Smart Grid* **2016**, *9*, 3102–3111, https://doi.org/10.1109/tsg.2016.2627339.

[26] PowerWorld version 22 (2021). power world corporation, Champaign, IL, USA. Available online: https://www.powerworld.com/download-purchase/demo-software (accessed on 15 June 2023).

[27] Sauer, P.W.; Pai, M. A.; Chow, J.H. Power System toolbox. In *Power System Dynamics and Stability: With Synchrophasor Measurement and Power System Toolbox,* Wiley-IEEE Press, 2017, pp.305–325, https://doi.org/10.1002/9781119355755.ch11.

Appendix

Table 5. Specified parameter values used for the simulated synchronous generator model for SMIB test system.

Inertia constant in p.u.	H	5
Damping factor in p.u.	D	0.05
Direct axis transient reactance in p.u.	x'_d	0.37
Mechanical input in p.u.	P_m	1

Table 6. Specified parameter values used for the simulated synchronous generator models for IEEE 9-bus system.

Damping factor in p.u.	D_1, D_2, D_3	4.73, 1.28, 0.60
Inertia constant in p.u.	H_1, H_2, H_3	2.3, 6.4, 3.01
Direct axis transient reactance in p.u.	$x'_{d1}, x'_{d2}, x'_{d3}$	0.06, 0.12, 0.18
Mechanical input in p.u.	P_{m1}, P_{m2}, P_{m3}	0.72, 1.63, 0.85

Table 7. Specified parameter values used for the simulated synchronous generator models for 19-generator 42-bus test system.

Damping factor in p.u.	D_1 to D_{19}	2
Inertia constant in p.u.	$H_1, H_2, H_3,$ $H_4, H_5, H_6,$ $H_7, H_8, H_9,$ $H_{10}, H_{11}, H_{12},$ $H_{13}, H_{14}, H_{15},$ $H_{16}, H_{17}, H_{18},$ H_{19}	4, 4.17, 4.23, 4.44, 4.38, 4.62, 2.50, 2.67, 4.11, 2.88, 3.83, 3.23, 5.1, 5.36, 5.40, 2.98, 4.82, 5.16, 3.80
Direct axis transient reactance in p.u.	x'_{d1} and x'_{d2} x'_{d3}, x'_{d6} and x'_{d17} x'_{d4} and x'_{d5} x'_{d7} to x'_{d17} x'_{d18} and x'_{d19}	0.25 0.37 0.25 0.25 0.25
Mechanical input in p.u.	P_{m1}, P_{m2}, P_{m3} P_{m4}, P_{m5}, P_{m6} P_{m7}, P_{m8}, P_{m9} $P_{m10}, P_{m11}, P_{m12}$ $P_{m13}, P_{m14}, P_{m15}$ $P_{m16}, P_{m17}, P_{m18}$ P_{m19}	0.95, 1.01, 0.85, 0.85, 0.85, 0.98, 0.98, 0.38, 0.51, 0.85, 0.87, 0.88, 0.69, 0.85, 0.91, 0.83, 0.52, 0.85, 0.88